Modeling and Visualization of Inter-Bone Distances in Joints

Ç. Demiralp, G. E. Marai, S. Andrews,
D. H. Laidlaw*, J. J. Crisco†
Brown University

C. Grimm‡
Washington University in St. Louis

1 Introduction

We demonstrate a method for visualizing inter-bone distances in articular joints. Visualization of inter-bone distances has the potential to characterize 3D structures and spatial relations non-invasively in complex joints. Our method uses both implicit and parametric representations of bones. The two types of representation have complementary strengths for different types of calculations. The implicit representation, the distance field, is a scalar field sampled on a regular grid. It specifies the signed distance from a point in the field to the nearest point on the bone. We calculate distance fields from the parametric representations which are smooth, locally controllable, manifold surface models [1] of the bones. These models are approximated from segmented CT scans of the bones [2].

We calculate inter-bone distances in a simple and efficient way with the help of the distance fields. We visually represent calculated inter-bone distances using color mapping and iso-contouring. We have found animations of these visualizations particularly helpful for understanding changes in relationships among bones. We applied our technique separately to three related joint structures of the hand – the distal radioulnar joint, the carpal bones of the wrist, and the scapholunate joint.

Although studies on structure and kinematics of joints have been done mostly *in vitro* using techniques such as soft tissue sectioning, electro-magnetic motion tracking and cadaveric CT scanning, studies using *in vivo* 3-D techniques have recently been introduced [3, 4, 5, 6]. To our knowledge, there has been no previous work using distance fields to represent bones, however distance fields have been used for other purposes in robotics [7] and computer graphics [8, 9]. The two scalar data visualization techniques we used, color mapping and iso-contouring, are well known scientific visualization techniques [10].

2 Materials and Methods

We capture 3D joint structures and kinematics using CT technology. Contours of bone surfaces are manually segmented from the set of 2D slices that comprise the CT images of the joint [3, 11, 12]. A bone surface is reconstructed by fitting a manifold surface to these contours [1], which results in a smooth, locally parameterized, C^2 continuous surface. The overlapped structure of the manifold surface representation, which is essentially inspired by differential geometry [13], has several advantages including flexibility in shape adjustments without costly constraints, and smooth transitions and uniformity among patches [1].

We compute distance fields for each bone using the reconstructed manifold bone models. A distance field is a scalar field which specifies the signed minimum distance from a point to the bone surface. The scalar field is stored as a sampled data set over a cuboid surrounding the bone. Sign is used to distinguish the inside from the outside of the bone. Keeping distance fields as an implicit representation has important advantages for geometric operations such as distance calculation, collision detection, level surface generation, performance of boolean operations, and inside/outside tests [8, 10]. We sample the distance fields in a regular 3D grid to speed look up.

*{cad, gem, stu, dhl}@cs.brown.edu
†Joseph_Crisco@brown.edu
‡cmg@cs.wustl.edu

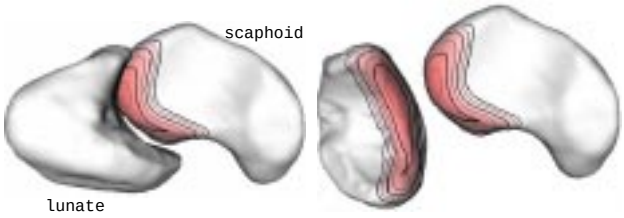

(a) (b)

Figure 1: A normal scapholunate joint. Bones are color mapped and contoured. The saturation of red (darker region in black and white, see [14] for the color version of this paper) on bone surfaces represents the distance to the nearest point on the opposite bone. Redder regions are closer. The maximum distance visualized is 5 mm. Contour lines are drawn at 0.5 mm intervals. (a) Bones in their correct anatomical context. (b) Bones rotated to show articulated surfaces more clearly.

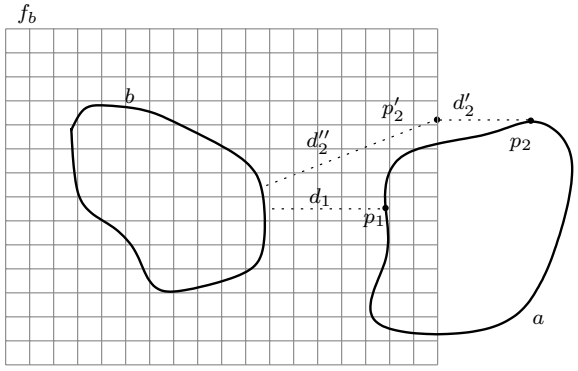

Figure 2: 2D illustration for obtaining distances from points p_1 and p_2 to bone b. f_b is the distance cuboid for bone b. Shortest distance values to bone b at the grid intersections are known. We use tricubic interpolation for values within the grid. Since p_1 is inside the cuboid, the distance from p_1 to b is equal to $f_b(p_1) = d_1$. For p_2, we first find the distance to the closest point p_2' in the distance cuboid and then the distance between p_2 and b is approximated as $d_2' + f_b(p_2') = d_2' + d_2''$.

2.1 Finding Inter-Bone Distances

Once distance fields are generated, we calculate the distance from an arbitrary point p to a bone surface b as follows. Each bone surface has a surrounding distance cuboid, over which the distance field is sampled. The point p can be inside or outside the distance cuboid f_b. Points outside the distance cuboid are far from the bone so they do not need to be accurate but do need to be smooth. We make sure that the region-of-interest areas (i.e., articulated surfaces) are well within the distance cuboid. Figure 2 illustrates the procedure. We evaluate two cases to find the distance:

p **is inside** f_b: we look up f_b for p,

p **is outside** f_b: we first find the distance to the nearest point p' on the boundary of f_b. We then add it to the distance value gathered by looking up f_b for p'.

We use tricubic B-spline interpolation to interpolate the sample values between grid locations. Note that, using the defined point-to-bone distance finding procedure, we find distances from every vertex in the surface model of one bone to every other neighboring bone. These distance values are updated for each frame of an animation based on the joint kinematics.

2.2 Visualization

We visualize distances using color mapping and contouring. Color maps are generated for each bone so that distance values of surface points are mapped to varying saturations of color (in this case the color is red). Colors that are more saturated represent shorter distances and colors that are less saturated represent longer distances.

Our contouring algorithm creates iso-lines on bone surfaces; each contour shows where the distance map is equal to a constant distance. For efficient computation and display, we assume that the distance map is linear over the triangular faces that comprise the surface of the bone, and, thus, the equal distance contours are straight line segments over each triangle. If the distance value of the contour d is within the range of the distance values at the vertices, a contour line segment is generated over the triangle [10].

Contouring becomes very useful for grouping distances and, in this sense, complements the color mapping technique. Distances beyond a threshold value are neither colored nor contoured. They are shown as a white surface. Figs 1 and 3 demonstrate the two techniques.

3 Results and Conclusion

We have implemented a prototype of our visualization technique described above in C++, using the Open Inventor graphics API on a SUN UltraSparc platform. We present results from three application examples: the comparison of normal and injured distal radioulnar joints (Figure 3), visualization of carpal kinematics and anatomy (see the accompanying video [15]), and study of scapholunate instability (Figure 1).

Joints are prone to injury and degenerative disease. In this paper we introduced a 3D inter-bone distance visualization method which can be used as a tool to explore hidden structures and subtle kinematics of joints non-invasively *in vivo*. The method uses an implicit model, a distance field, as well as a parametric surface model for each bone. We demonstrated its application to the distal radioulnar joint, the carpal bones of the wrist, and the scapholunate joint. Preliminary results show that our method could be very useful in the study of normal anatomy and kinematics of complex joints like the wrist. A prototype of this visualization will be exhibited at the upcoming American Society for Surgery of the Hand Meeting [16]. Our technique may also have applications to the study of wrist disorders such as rheumatoid arthritis, inter-carpal ligament tear/attenuation, and carpal-tunnel syndrome.

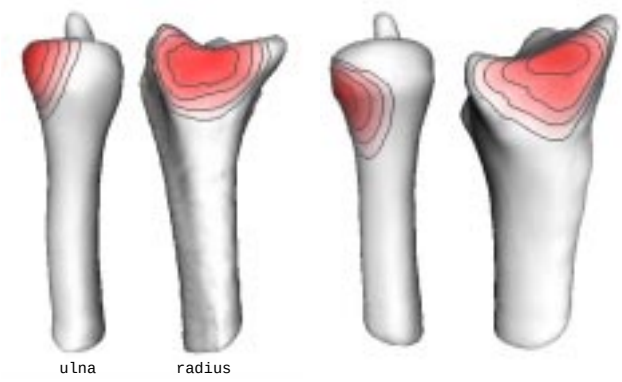

(a) Right (b) Left (mirrored)

Figure 3: (a) Pronated normal distal radioulnar joint (right forearm). (b) Pronated injured distal radioulnar joint (left forearm of the same patient). The left forearm was mirrored for ease of comparison. Note the evident shift in the location of the articulation area. The saturation of red on bone surfaces represents the distance to the nearest point on the opposite bone. Redder regions are closer. Bones are rotated to show the articulated surfaces more clearly. The maximum distance visualized is 5mm; contour lines are drawn at 1mm intervals.

Acknowledgments

Thanks to Daniel Acevedo and Rosemary M. Simpson for their help with the video. Thanks also to Eileen L. Vote for her careful reading and suggestions. This work was partially supported by NIH (AR-44005) and NSF (CCR-0093238). Opinions expressed in this paper are those of the authors and do not necessarily reflect the opinions of NSF.

References

[1] C. Grimm and J. Hughes. Modeling surfaces of arbitrary topology using manifolds. In *SIGGRAPH 95 Conference Proceedings*, pages 359–368, 1995.

[2] C. Grimm, D. H. Laidlaw, and J. J. Crisco. Fitting manifold surfaces to 3d point clouds. *Journal of Biomechanics*. Accepted.

[3] J. J. Crisco, R. D. McGover, and S. W. Wolfe. 3-d in-vivo kinematics of the distal radioulnar joint in malunited distal radius fractures. *Journal of Orthopedic Research*, 17:96–100, 1999.

[4] F. Eckstein, A. Gavazzeni, H. Sittek, M. Haubner, A. Losch, S. Milz, K. H. Englmeier, E. Schulte, R. Putz, and M. Reiser. Determination of knee joint cartilage thickness using threedimensional magnetic resonance chondro-crassometry (3d mr-ccm). *Magn.Reson.Med.*, 36:256–265, 1996.

[5] V. Feipel, M. Rooze, S. Louryan, and M. Lemort. Bi- and three-dimensional ct study of carpal bone motion in lateral deviation. *Surg Radiol Anat*, 14:381–389, 1992.

[6] S. L. Van Sint Jan, G. J. Clapworthy, and Marcel Rooze. Visualization of combined motions in human joints. *IEEE Computer Graphics and Applications*, pages 10–14, November/December 1998.

[7] R. Kimmel, N. Kiryati, and A. Bruckstein. Multi-valued distance maps for motion planning on surfaces with moving obstacles. *IEEE Transactions on Robotics & Automation*, 14:427–436, 1998.

[8] S. F. Frisken, R. N. Perry, A. P. Rockwood, and T. R. Jones. Adaptively sampled distance fields: A general representation of shape for computer graphics. In *SIGGRAPH 2000 Conference Proceedings*, 2000.

[9] A. Gueziec. Meshsweeper: Dynamic point-to-polygonal-mesh distance and applications. *IEEE Transactions on Visualization and Computer Graphics*, 7(1):47–61, 2001.

[10] K. Martin W. Schroeder and Bill Lorensen. *The Visualization Toolkit: An Object-Oriented Approach to 3D Graphics*. Prentice Hall, 1997.

[11] D. C. Moore, K. A. Hogan, J. J. Crisco, E. Akelman, M. F. DaSilva, and A-P. C. Weiss. 3-d in-vivo kinematics of the distal radioulnar joint in malunited distal radius fractures. In *Orthopedic Research Society 46th Annual Meeting*, Orlando, Florida, March 12-15 2000.

[12] S. L. Pike, D. L. Galvin, S. W. Wolfe, A-P. C. Weiss, E. Akelman, and J. J. Crisco. Carpal kinematics are abnormal in both wrists of patients with unilateral scapholunate interosseous ligament injuries. In *12th Conference of the European Society of Biomechanics*, Dublin, 2000.

[13] M. Spiviak. *Differential Geometry*. Publish or Perish, Houston, TX, 1979.

[14] http://www.cs.brown.edu/research/graphics/research/pub/papers/distviz01.pdf.

[15] http://www.cs.brown.edu/research/graphics/research/sciviz/hand/video.html.

[16] J.J. Crisco, C. Demiralp, D. H. Laidlaw, A-P. C. Weiss, E. Akelman, and S.W. Wolfe. Interactive visualization of 3d carpal kinematics and bony anatomy. In *American Society for Surgery of the Hand 56th Annual Meeting Abstracts*, Maryland, October 2001.